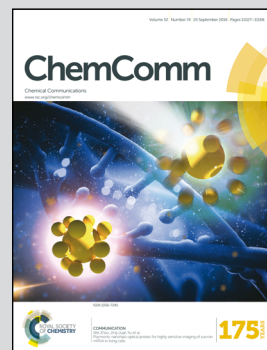


**Showcasing research from Drs Yoshida & Akimoto's laboratory,
Department of Materials Engineering at the University of Tokyo,
Japan**

**A surface-grafted thermoresponsive hydrogel in which the
surface structure dominates the bulk properties**

A surface-grafted hydrogel, in which the surface structure dominates the bulk properties, was successfully synthesized by immobilization of the ATRP initiator at the surface of the gel and the subsequent ARGET ATRP step.

As featured in:



See Aya Mizutani Akimoto,
Ryo Yoshida *et al.*,
Chem. Commun., 2016, 52, 11064.



www.rsc.org/chemcomm

Registered charity number: 207890



Cite this: *Chem. Commun.*, 2016, 52, 11064

Received 23rd May 2016,
Accepted 21st July 2016

DOI: 10.1039/c6cc04307k

www.rsc.org/chemcomm

A surface-grafted thermoresponsive hydrogel in which the surface structure dominates the bulk properties†

Ko Matsukawa, Tsukuru Masuda, Aya Mizutani Akimoto* and Ryo Yoshida*

A surface-grafted hydrogel was successfully synthesized by immobilization of the ATRP initiator at the surface region of the gel and the subsequent ARGET ATRP step. This is the first example of a bulk hydrogel with a dense surface-localized layer of a grafted polymer and “active” permeation control of the gel.

Polymer hydrogels are “open systems”, *i.e.* physical and chemical signals can easily enter the networks. They are composed almost entirely of water, and have elastic moduli similar to those of biological materials. Because of these properties, many gel functions such as stimuli-responsiveness,^{1–3} high mechanical strength,^{4–6} self-healing,^{7,8} molecular recognition,^{9,10} and self-oscillation^{11–14} have been developed. In many cases, these functions have been obtained by the precise design of the homogeneous bulk polymer network structure at the nano-scale, which has become possible due to advances in polymer synthesis.^{4,15,16} However, few studies have been carried out on the effect of surface functionalization of hydrogels.¹⁷ Because many important hydrogel phenomena, including permeation, friction, and adhesion, occur through or at the surface of a hydrogel, surface functionalization may be a highly effective method to add novel functionality to hydrogels.

Recently, polymer surface-modification techniques have been advanced by the development of living radical polymerization (LRP). Atom-transfer radical-polymerization (ATRP) is a class of LRP and is widely used for the preparation of well-defined polymer grafted surfaces on solid substrates.¹⁸ Furthermore, an activator regenerated by electron transfer for ATRP (ARGET ATRP) has been developed to overcome the problems and limitations of ATRP such as sensitivity to oxygen and the need for a high copper catalyst concentration.¹⁹ Simakova *et al.* succeeded in the

controlled synthesis of poly(oligo(ethylene oxide) methyl ether methacrylate) in aqueous media with a very low concentration of a Cu catalyst,²⁰ and Matyjaszewski *et al.* reported the preparation of well-defined and highly dense polymer brushes on silicon wafers without the need for special equipment or deoxygenation using a surface-initiated ARGET ATRP method.²¹ Because ARGET ATRP can proceed in water without the need for solvent deoxygenation and with a low Cu concentration, it is a powerful tool for the surface-modification of water-based materials, including hydrogels.

In this study, we prepared a novel surface-grafted gel that has polymer chains grafted onto a localized surface region of a bulk hydrogel by surface-initiated ARGET ATRP. ATRP initiators can be introduced locally in the surface region by introducing the initiator in a poor solvent because a gel shrinks in a poor solvent and penetration of initiators into a gel network is suppressed.²² For our first trial to create a surface grafted gel, we selected the thermoresponsive polymer poly(*N*-isopropylacrylamide) (PNIPAAm), which is widely used in various biomedical applications,^{23,24} for the main and the grafted chains of the gel (Fig. 1). The thermoresponsive kinetics of the prepared gel was compared with that of a conventional PNIPAAm gel (non-grafted gel).

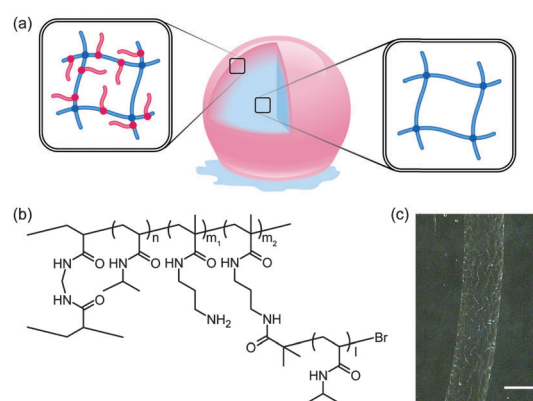


Fig. 1 (a) Schematic image, (b) chemical structure and (c) appearance in the equilibrium state (scale bar: 1 mm) of the SG gel.

Department of Materials Engineering, School of Engineering,
The University of Tokyo, 7-3-1 Hongo, Bunkyo-ku, Tokyo, 113-8656, Japan.

E-mail: akimoto@cross.t.u-tokyo.ac.jp, ryo@cross.t.u-tokyo.ac.jp;

Fax: +81-3-5841-7112; Tel: +81-3-5841-7112

† Electronic supplementary information (ESI) available: Experimental details, DSC, fluorescence microscopy and video of the shrinking process. See DOI: 10.1039/c6cc04307k



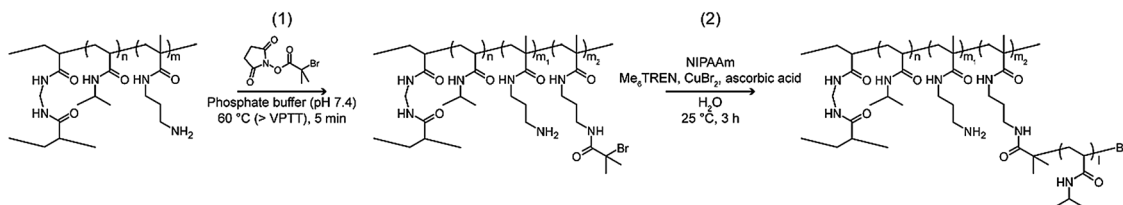


Fig. 2 Schemes for (1) the immobilization of the NHS-initiator onto the surface of the gel, and (2) PNIPAAm grafting onto the surface of the gel.

First, cylindrical hydrogels (diameter = 1.02 mm) composed of NIPAAm, *N*-(3-aminopropyl)methacrylamide (NAPMAm), and *N,N'*-methylenebisacrylamide (MBAAm) (NIPAAm : NAPMAm : MBAAm = 95 : 2 : 3 (mol ratio)) were synthesized by redox radical polymerization using ammonium persulfate and *N,N,N',N'*-tetramethylethylenediamine. Then ATRP initiators were immobilized only onto the surface region of gels by immersing gels in phosphate buffer solution (pH 7.5) including the active ester functionalized ATRP initiator at higher temperature than volume phase transition temperature (VPTT) for a short time (5 min). After that, PNIPAAm grafted polymers were introduced by grafting-from ARGET ATRP in aqueous solution (Fig. 2 and Fig. S1 (ESI[†]) for the illustration of the synthetic process). The obtained surface-grafted gels (SG gel) were colorless but had many fine wrinkles on the surface at equilibrium at 25 °C, while the surface of the non-grafted gels (NG gel) was smooth. These wrinkles are attributed to a mismatch between the swelling ratio of the interior and the surface of the SG gel. To determine the LCST of the grafted polymer and VPTT of the polymer network, DSC measurements were conducted for both SG and NG gels. The SG gel had two endothermic peaks during heating; one at 33.7 °C due to the PNIPAAm-grafted polymer and one at 41.2 °C due to the poly(NIPAAm-*r*-NAPMAm) polymer network, the former of which was not observed for the NG gel (Fig. S2, ESI[†]). The DSC results indicate that the introduction of grafted polymers onto the gel by ARGET ATRP successfully occurred. The spatial distribution of grafted polymers was also evaluated by copolymerizing a fluorescent monomer in grafted polymers and subsequent fluorescence microscopy of the cut face of the obtained gels. The fluorescence intensity of the surface region (approximately 200 μm) was higher than that of the inside

region (Fig. S3, ESI[†]), indicating that the grafted polymer was grafted with high density in the surface region of the gel.

To investigate the effect of surface polymer grafting on the volume phase transition behaviour of the thermoresponsive gels, the swelling ratios of NG and SG gels were measured in water after keeping them at each temperature for 1 hour. The NG gel, which is a conventional poly(NIPAAm-*co*-NAPMAm) gel, showed an LCST type volume phase transition behaviour, with isotropic shrinkage at temperatures greater than 35–40 °C. In contrast, the SG gels had a two-phase coexistence at temperatures around 40–45 °C, where both swollen and shrunken states were observed simultaneously in the same gel (Fig. 3(a–c)). This unique phase separation pattern is similar to the “bubble pattern” that can be observed in the phase transition of acrylamide hydrogels upon immersion in an acetone–water mixture, a poor solvent for acrylamide gels. In this phenomenon, the diffusion of solvent molecules through the surface is restricted due to the formation of a dense skin layer on the surface of the gel.²⁵ Thus, when the temperature increases above the VPTT, the diffusion of water molecules through the SG gel was restricted. After the “bubble pattern” phase, the swollen area of the SG gel suddenly cracked and shrank at around 45 °C. This result suggests that the dehydration and aggregation of the crosslinked polymer network progressed during the two-phase coexistence, and stress gradually increased, leading to the formation of a skin on the dehydrated grafted polymer network. When this stress exceeded the mechanical strength of the grafted polymer network, cracks formed. After the cracking, rapid shrinkage occurred due to exposure of the non-grafted, inside region of the gel.

To analyse the shrinking behaviour of the gels in more detail, the NG and SG gels were immersed in an aqueous solution

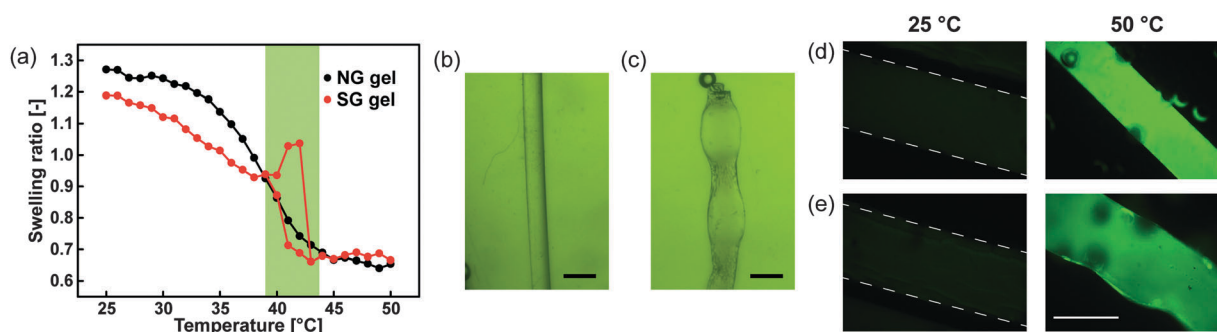


Fig. 3 (a) Swelling ratio of the NG (black dots) and SG gels (red dots) over the studied temperature range. (b) NG gel and (c) SG gel observed using an optical microscope close to the VPTT. Scale bar: 1 mm. Fluorescence images of (d) the NG gel and (e) the SG gel at 25 °C (left) and 50 °C (right) in an aqueous ANS solution.



containing ANS (1 mg L^{-1}) and observed by fluorescence microscopy. ANS fluoresces only when the surrounding environment is hydrophobic. Thus, hydration/dehydration of the polymer network can be visualized by fluorescence microscopy. Fig. 3(d and e) shows the fluorescence microscopy images of NG and SG gels at 25°C (below the VPTT) and at 50°C (above the VPTT). Below the VPTT (25°C), both gels were in a swollen state and did not exhibit fluorescence. On the other hand, above the VPTT (50°C), the SG gel maintained its swollen state but fluoresced slightly, while the NG gel shrank and fluoresced strongly from the whole gel. These results indicate that the SG gel formed a dense skin layer upon dehydration of the grafted polymer network and restricted solvent diffusion, while the NG gel did not form a skin layer. Generally, the PNIPAAm gel cross-linked by a conventional low molecular weight crosslinker forms a skin layer above the VPTT. However, because the NG gel was sufficiently small and highly hydrophilic due to copolymerization with hydrophilic NAPMAM, it didn't form a skin layer. Previous studies have shown that when a thermoresponsive, grafted polymer is introduced homogeneously throughout the thermoresponsive gel network (so-called comb-type grafted gels), rapid shrinkage occurs due to the hydrophobic interactions between rapidly dehydrated grafted polymer chains and crosslinked polymer main chains.²⁶ On the other hand, in the case of the surface-grafted gel, the formation of a dense skin layer was induced even in the small gel with a particular composition that did not originally form a skin layer, instead of the rapid shrinkage. This skin layer formed due to the rapid dehydration of the grafted polymer chains introduced locally in the surface region. Although there have been numerous reports on the control of solvent diffusion using the gel skin layers, including drug delivery systems and sensors,^{27,28} several problems persist; for example, the formation of a skin layer strongly depends on the chemical composition and size of the gel, and it is very difficult to completely control the formation and deformation of the skin layer. This surface-grafted gel has the potential to remove these limitations and make skin layers more easily accessible.

To evaluate the effect of skin layer formation attributed to surface-grafting on the kinetics of shrinking and swelling behaviour of the thermoresponsive gel, a sudden temperature increase was applied to both the NG and SG gels, and the time evolution of the swelling ratios was measured. The change in gel diameter with time during shrinkage is shown in Fig. 4 and Movie S1 (ESI†). The NG gel rapidly shrank immediately after temperature increase, without the formation of a skin layer, and an almost totally shrunken state was obtained after 15 min. In contrast, the SG gel maintained a swollen state for a defined period due to the formation of a dense skin layer. Furthermore, approximately 15 minutes after the temperature increase, a crack suddenly formed on the surface of the gel and it started to shrink rapidly. This crack appeared because the graft-polymer network of the gel was not able to sustain the tension generated by the crosslinked polymer network inside the gel; this is the same phenomenon observed in the temperature dependent swelling measurements (Fig. 3(a)). However, if the timing of cracking and shrinkage can be controlled, surface-grafted gels

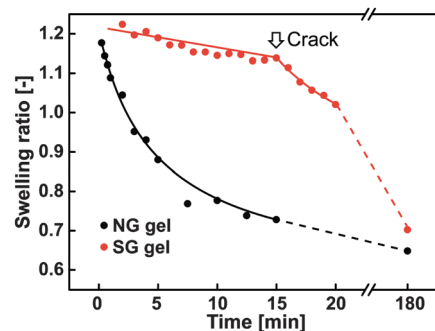


Fig. 4 The change in the diameter of the NG (black) and SG gels (red) with time during the shrinking process induced by a temperature increase ($25 \rightarrow 40^\circ\text{C}$).

could be used as microvalves and drug carriers that respond with a time lag. The time evolution of the gel diameter and diameter ratio (d_n) during the swelling process is shown in Fig. 5. d_n is calculated for a cylindrical gel using eqn (1). d_∞ and d_0 are the diameter ratio in the equilibrium state and at time zero, respectively. The relationship among d_n , time t and the relaxation time τ can also be written as follows.

$$d_n = \frac{d_\infty - d(t)}{d_\infty - d_0} \propto e^{-\frac{t}{\tau}} \quad (1)$$

The relationship between τ and the cooperative diffusion coefficient (D), the elastic modulus of the polymer network (K) and the friction between the polymer network and the solvent molecules (f) can be written as follows.

$$D = \frac{3d_\infty^2}{8\pi^2\tau} = \frac{K}{f} \quad (2)$$

In the case of the NG gel, a relaxation mode was observed during swelling at $\tau = 32 \text{ s}$. On the other hand, the SG gel showed slower swelling ($\tau = 42 \text{ s}$) than that of the NG gel. Slow relaxation might be attributed to large friction between the dense polymer network in the surface region and the solvent molecules which diffused through the surface region into the gel; the large f results in small D by eqn (2). This slow relaxation in particular shows that the physical structure of the surface region dominates the properties of the bulk gel. Future work will involve a detailed investigation of the gels under various conditions to yield important results regarding the gel properties and develop strategies for the physical control of the gel network.

A surface-modified hydrogel was successfully synthesized by immobilization of the ATRP initiator at the surface region of the gel and the subsequent ARGET ATRP step. To our best knowledge, this is the first example of a bulk hydrogel with a dense surface-localized layer of grafted polymers and "active" permeation control of the gel. It was revealed that the grafted polymers in the gel had been introduced into the gel surface region by using a fluorescent co-monomer as a probe of the grafted polymers. From optical and fluorescence microscopy observations at several temperatures, a two-phase coexistence was observed, suggesting the formation of a dense skin layer at the surface of the gel; this occurred because the grafted



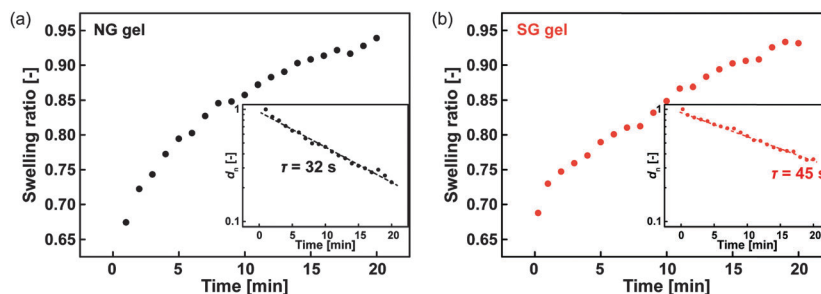


Fig. 5 Change in the diameter of the (a) NG and (b) SG gels with time during the swelling process induced by a temperature decrease ($40 \rightarrow 25^\circ\text{C}$). Inset in each graph: plots of d_n against time, and the relaxation time from the slope of the straight line.

polymer induced fast shrinkage of the polymer network in the surface region. During temperature-induced shrinkage, the surface-grafted gel maintained a swollen state for a defined time due to the formation of a dense skin layer; however, it then shrank rapidly and cracked because the inner stress exceeded the mechanical strength of the dehydrated polymer network. In contrast, the surface-grafted gel showed a slow relaxation in the swelling process, which was caused by the high friction between the highly dense polymer network and solvent molecules. Here, we have discussed about the unique behaviours of the surface-grafted gel which has a thermosensitive polymer network and thermosensitive grafted polymers. Considering that there are hundreds of possible combinations of polymer species, these surface-grafted gels have great potential for applications such as functional microvalves, non-dryable water containers, and controlled release carriers.

This work was supported in part by a research fellowship to K. M. from the Japan Society for the Promotion of Science through the Program for Leading Graduate Schools (MERIT), a research fellowship to T. M. from the Japan Society for the Promotion of Science for Young Scientists (No. 14J09992), and a Grant-in-Aid for Scientific Research to R. Y. from the Ministry of Education, Culture, Sports, Science, and Technology of Japan (Grant No. 15H02198). We are grateful to Dr Younsoo Kim and Prof. Takuzo Aida (The University of Tokyo) for use of a DSC instrument, and Dr Masamichi Nakayama (Tokyo Women's Medical University) for teaching us the synthesis of FLAAM.

Notes and references

- 1 F. Liu and M. W. Urban, *Prog. Polym. Sci.*, 2010, **35**, 3.
- 2 B. Jeong and A. Gutowska, *Trends Biotechnol.*, 2002, **20**, 305.
- 3 L. Klouda and A. G. Mikos, *Eur. J. Pharm. Biopharm.*, 2008, **68**, 34.
- 4 J. P. Gong, Y. Katsuyama, T. Kurokawa and Y. Osada, *Adv. Mater.*, 2003, **15**, 1155.
- 5 K. Haraguchi, T. Takehisa and S. Fan, *Macromolecules*, 2002, **35**, 10162.
- 6 J. Sun, X. Zhao, W. R. K. Illeperuma, O. Chaudhuri, K. H. Oh, D. J. Mooney, J. J. Vlassak and Z. Suo, *Nature*, 2012, **489**, 133.
- 7 M. Nakahata, Y. Takashima, H. Yamaguchi and A. Harada, *Nat. Commun.*, 2011, **2**, 511.
- 8 M. Zhang, D. Xu, X. Yan, J. Chen, S. Dong, B. Zheng and F. Huang, *Angew. Chem., Int. Ed.*, 2012, **51**, 7011.
- 9 H. Yamaguchi, Y. Kobayashi, R. Kobayashi, Y. Takashima, A. Hashizume and A. Harada, *Nat. Commun.*, 2012, **3**, 603.
- 10 A. Harada, Y. Takashima and M. Nakahata, *Acc. Chem. Res.*, 2014, **47**, 2128.
- 11 T. Masuda, A. Terasaki, A. M. Akimoto, K. Nagase, T. Okano and R. Yoshida, *RSC Adv.*, 2015, **5**, 5781.
- 12 T. Ueki and R. Yoshida, *Phys. Chem. Chem. Phys.*, 2014, **16**, 10388.
- 13 Y. Shiraki, A. M. Akimoto, T. Miyata and R. Yoshida, *Chem. Mater.*, 2014, **26**, 5441.
- 14 S. Nakata, M. Yoshii, S. Suzuki and R. Yoshida, *Langmuir*, 2014, **30**, 517.
- 15 Y. Okumura and K. Ito, *Adv. Mater.*, 2001, **13**, 485.
- 16 T. Sakai, T. Matsunaga, Y. Yamamoto, C. Ito, R. Yoshida, S. Suzuki, N. Sasaki, M. Shibayama and U. Chung, *Macromolecules*, 2008, **41**, 5379.
- 17 J. P. Gong, T. Kurosawa, T. Narita, G. Kagata, Y. Osada, G. Nishimura and M. Kinjo, *J. Am. Chem. Soc.*, 2001, **123**, 5582.
- 18 K. Matyjaszewski, *Macromolecules*, 2012, **45**, 4015.
- 19 W. Jakubowski and K. Matyjaszewski, *Macromolecules*, 2006, **39**, 39.
- 20 A. Simakova, S. E. Averick, D. Konkolewicz and K. Matyjaszewski, *Macromolecules*, 2012, **45**, 6371.
- 21 K. Matyjaszewski, H. Dong, W. Jakubowski, J. Pietrasik and A. Kusumo, *Langmuir*, 2007, **23**, 4528.
- 22 A. Mizutani, K. Nagase, A. Kikuchi, H. Kanazawa, Y. Akiyama, J. Kobayashi, M. Annaka and T. Okano, *J. Chromatogr. B: Anal. Technol. Biomed. Life Sci.*, 2010, **878**, 2191.
- 23 K. Nagase, J. Kobayashi, A. Kikuchi, Y. Akiyama, H. Kanazawa and T. Okano, *Langmuir*, 2008, **24**, 511.
- 24 Y. Hiruta, M. Shimamura, M. Matsuura, Y. Maekawa, T. Funatsu, Y. Suzuki, E. Ayano, T. Okano and H. Kanazawa, *ACS Macro Lett.*, 2014, **3**, 281.
- 25 E. S. Matsuo and T. Tanaka, *Nature*, 1992, **358**, 482.
- 26 R. Yoshida, K. Uchida, Y. Kaneko, K. Sakai, A. Kikuchi, Y. Sakurai and T. Okano, *Nature*, 1995, **374**, 240.
- 27 A. Matsumoto, T. Ishii, J. Nishida, H. Matsumoto, K. Kataoka and Y. Miyahara, *Angew. Chem., Int. Ed.*, 2012, **51**, 2124.
- 28 B. Beier, K. Musick, A. Matsumoto, A. Panitch, E. Nauman and P. Irazoqui, *Sensors*, 2011, **11**, 409.

